Research Article | Vol. 27, No. 3 | 4 Feb 2019 | OPTICS EXPRESS 3200
Optics EXPRESS

Two-color surface plasmon resonance nanosizer for gold nanoparticles

Quaid Zaman,[1] Jefferson Souza,[2] Omar Pandoli,[3] Karlo Q. Costa,[2] Victor Dmitriev,[2] Daniele Fulvio,[1] Marco Cremona,[1] Ricardo Q. Aucelio,[3] Giselle Fontes,[4] and Tommaso Del Rosso[1,*]

[1]*Department of Physics, Pontifícia Universidade Católica do Rio de Janeiro, Rua Marques de São Vicente, 22451- 900, Rio de Janeiro, Brazil*
[2]*Department of Electrical Engineering, Federal University of Para, Institute of Technology, Belem 66075-110, Brazil*
[3]*Department of Chemistry, Pontifícia Universidade Católica do Rio de Janeiro, Rua Marques de São Vicente, 22451-900, Rio de Janeiro, Brazil*
[4]*Division of Metrology of Materials, National Institute of Metrology Quality and Technology - INMETRO, Duque de Caxias, RJ 25250-020, Brazil*
[*]*tommaso@puc-rio.br*

Abstract: We study the potentialities of a two-color Surface Plasmon Resonance (SPR) spectroscopy nanosizer by monitoring the assembling of a colloidal dispersion of citrate stabilized gold nanoparticles (AuNPs) on SiO_2 surface. When the AuNPs/water composite's optical density layer is negligible and the electron mean-free path limitation is taken into account in the AuNPs' dielectric constant;s formulation, the surface density σ of the nanoparticle array and the statistical mean size <r> of the nanoparticles can be straightly determined by using two-color SPR spectroscopy in the context of Maxwell's Garnett theory. The optical method, demonstrated experimentally for AuNPs with a nominal mean diameter of 15 nm, can, theoretically, be extended to bigger nanoparticles, based on a simple scaling relation between the extinction cross section of the single nanoparticle σ_{ext} and the surface density σ. The experimental results, comparable to those obtained by AFM, transmission electron microscopy and dynamic light scattering technique, establish a novel insight on the SPR spectroscopy's potential to accurately characterize nanomaterials.

1. Introduction

Gold nanoparticles (AuNPs) play a crucial role in the expansion of nanotechnology to the market of diagnostic systems and other applications [1]. This particular role of the AuNPs is due to their very high chemical stability when compared to silver or copper counterparts, also characterized by a localized surface plasmon resonance (LSPR), but presenting instability with time caused by oxidation of the metals [1]. The measurement of the dimensions of the AuNPs, and generally of metal and dielectric nanoparticles, can be performed in liquid form by the dynamic light scattering (DLS) technique [1], or in solid state using the transmission electron microscopy (TEM) or the atomic force microscopy (AFM) [2]. The results of DLS are influenced by formation of a double layer, caused by the surface species bound to the metal core or solvent and solutes molecules solvating the nanoparticles [2]. TEM investigation is the most effective, since it allows determination of the statistical dimensions, shape and chemical nature (metallic, organic) of the nanomaterial, but it is also the most expensive [2]. AFM is particularly attractive for the measurement of the average height of nanomaterials, since lateral resolution is limited by the dimension of the tip probe, generally of the order of 10 nm [2].

Recent applications of AuNPs in SPR spectroscopy are aimed to the enhancement of the resolution of optical biosensors using the metal nanoparticle-amplified SPR spectroscopy

#349488 https://doi.org/10.1364/OE.27.003200
Journal © 2019 Received 20 Nov 2018; revised 18 Jan 2019; accepted 18 Jan 2019; published 30 Jan 2019

Optics EXPRESS

(PA-SPR) configuration [3,4]. In PA-SPR spectroscopy, likewise in surface enhanced Raman scattering (SERS) spectroscopy based on bidimensional arrays of AuNPs [5], it is fundamental to know both the surface density (σ) and dimension of the nanoparticles in order to calculate the mass resolution of the sensor [3] or SERS gain [5], respectively. SPR spectroscopy studies on self-assembled monolayers (SAM) of AuNPs in the Kreschtmann configuration show that the dielectric constant of the Au/water composite film can be measured once that σ and the size of the AuNPs are determined by complementary techniques [4,6]. Depending on the dimension of the AuNPs and excitation wavelength, when σ is high, or the SiO_2, interlayer thickness is below 5 nm, inter AuNPs dipole-dipole interactions and dipole interaction between the Au thin film and the AuNPs have to be considered. In this case, numerical or semianalitical optical models taking into account the optical anisotropy of the AuNPs have to be used for the accurate determination of σ [4,7].

In the present research we show how SPR spectroscopy can be used for the development of a two-color SPR nanosizer, able to measure both the statistical mean radius $<r>$ and the surface density σ of citrate stabilized AuNPs deposited over SiO_2 surfaces [8]. These performances are possible when the optical density $\tau(\lambda,\sigma)$ of the SAM of AuNPs is negligible at both the excitation wavelengths. The latter condition is realized by minimizing the surface density σ of the bidimensional array of AuNPs and the overlap between the single nanoparticle extinction cross-section and the frequency of the laser source used to excite the SPPs. The value of $<r>$ measured by SPR spectroscopy is compared with the results obtained by traditional techniques such as AFM, TEM and DLS. The accuracy of the optical method is evaluated taking in consideration different experimental parameters, such as the uncertainty in the experimental values of the thickness and complex dielectric constant of the thin films composing the SPR sensing platforms, the nanoparticle surface density σ, and the experimental polidispersitivity of the colloidal solution of AuNPs. Finally, we present a detailed discussion about the limits of the applicability of the presented method to gold nanoparticles of different sizes.

2. Materials and experimental methods

Prior to SPR monitoring, the colloidal dispersion of AuNPs has been characterized by a Tecnai Spirit Transmission Electron Microscope (FEI Company) operating at 30 kV with bright-field detector, by DLS spectroscopy (HORIBA, Nanoparticles analyzer, model SZ-100-Z), AFM microscopy (Bruker, Multimode 8) in Tapping Mode with ScanAsyst-Air tips (spring constant ≈0,4 N/m) and UV-Vis spectroscopy (Perkin Elmer, Lambda 950).

The SPR sensing platforms were prepared by silanization of SF_4 glass slides via (3-mercaptopropyl) trimethoxysilane (MPTS) to form a self-assembling layer for the adhesion of gold thin film of 50 nm thickness, like reported in [9]. Prior to the deposition of SiO_2, a molecular 2D silica-like surface was formed by self-assembling of MPTS on gold thin film followed by hydrolysis and condensation process [10,11]. The thin films of gold and SiO_2, the latter with a nominal thickness of about 30 nm, were deposited using a Leybold Univex 450 e-beam gun system in high vacuum environment (2×10^{-6} mbar) at a rate of 2 Å/sec. The external SiO_2 thin film was functionalized with a self-assembled monolayer of 3-Aminopropyltriethoxysilane (APTMS) [5,6], which acts as a Coulombic ligand for negative charged citrate stabilized AuNPs. The AuNPs were synthesized in this work using the chemical procedure described in [8] adapted to obtain statistical mean diameter of about 15 nm.

Figure 1 represents the two-color SPR nanosizer in the Kreschtmann configuration, with double laser sources at the wavelengths of 633 nm (Thorlabs U.S.A, He-Ne, 5 mW) and 783 nm (Ondax U.S.A, model LM-783-PLR-75-1, 75 mW), and a continuous flux pump (FutureChemistry, Netherlands) for AuNPs-SAM deposition and sensor rinsing. The SF4/Au/SiO_2 sensing platform is optically coupled to the SF4 prism through a refractive index matching oil (n = 1.75, Cargille Laboratories, USA).

Optics EXPRESS

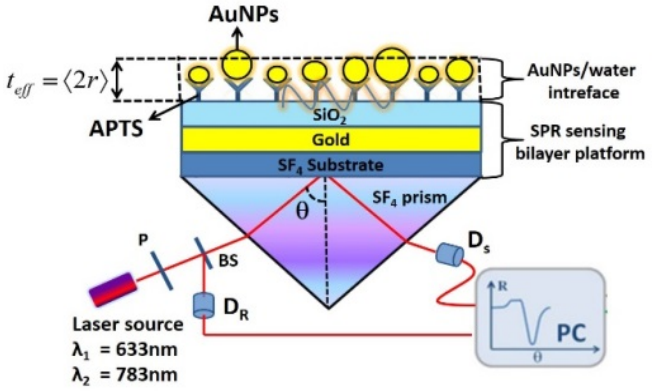

Fig. 1. Two-color SPR nanosizer in the Kreschtmann configuration. The thickness of the nanocomposite layer t_{eff} is considered equal to the statistical mean diameter $<2r>$ of the AuNPs.

The experimental procedure necessary for the correct application the two-color SPR nanosizer to citrate stabilized AuNPs of unknown dimension can be divided in the following steps:

a) evaluation of the spectral overlap between the extinction cross-section of the AuNPs and the wavelength λ_1 and λ_2 of the excitation laser sources.

b) Accurate measurement of the dielectric constant and thickness of the gold and SiO_2 thin films constituting the SPR sensing platform, at both wavelengths λ_1 and λ_2.

c) Deposition of SAM of AuNPs with sufficiently low optical density τ.

d) Analysis of the experimental data applying the two-color SPR method supported by MG theory in the low surface density approximation.

3. Theoretical model and working principle of two-color SPR nanosizer

For modelling of the dielectric constant $\varepsilon_{NP} = \varepsilon' + i\varepsilon''$ of the colloidal dispersion of AuNPs, we take into account the electron mean free path limitation [12], and modify the traditional Johnson and Christy [13] datasheet values using the analytical procedure described in [12]. Since the quantum size effects appear only for AuNPs with diameter smaller than ~2 nm, the mean free path limitation is valid for the nanoparticles analysed in the present work [14]. To model the optical response of an array of metal or dielectric NPs embedded in a non-absorbing external medium with dielectric constant ε'_m, we use the formulation of the modified Maxwell-Garnett effective medium theory reported in [6,15]. The latter, includes in the formulation of the effective dielectric function of the composite thin film ε_{eff} the effects due to particle geometry and dimension, valid for AuNPs with a diameter up to 50 nm [15].

In this theoretical frame the effective dielectric function of a the Au/external medium composite layer $\varepsilon_{eff} = (\varepsilon'_{eff} + i\varepsilon''_{eff})$ is written as follows:

$$\varepsilon'_{eff} = \varepsilon'_m + \frac{AC + BD}{C^2 + D^2} \text{ and } \varepsilon''_{eff} = \frac{BC - AD}{C^2 + D^2}, \quad (1)$$

In case of spherical AuNPs with negligible dipole-dipole collective interaction, the capital letter symbols of Eq. (1) can be simplified as:

$$A = f\left(\varepsilon' - \varepsilon'_m\right), \quad B = f\,\varepsilon'', \quad (2)$$

Optics EXPRESS

$$C = \varepsilon_m' + (\varepsilon' - \varepsilon_m')/3 - f(\varepsilon' - \varepsilon_m')/3\varepsilon_m', \tag{3}$$

$$D = \varepsilon''/3 - f\varepsilon''/3\varepsilon'. \tag{4}$$

In the equations above, the parameter f is the metallic volume fraction of the composite layer with the thickness $t_{eff} = < 2r >$, where $< 2r >$ is the statistical mean of the distribution of the diameter of the AuNPs, as sketched in Fig. 1.

In the initial stage, we suppose the colloidal solution to be perfectly monodispersed, with the nanoparticles having all the same radius equal to $< r >$. With this approximation whose validity will be discussed later, the parameter f can be expressed as $f = 2\pi < r >^2 /3 < d >^2$,where $< d >$ represents the statistical average distance between the AuNPs on the SiO_2 surface. For non-interacting AuNPs, the exact spatial distribution of the bidimensional array of AuNPs deposited over the SiO_2 substrate does not influence on the optical response of the device. The latter depends only on the parameter f, linked to the surface density σ of AuNPs by the simple relation $f = 2\pi\sigma < r >^2 /3$.

In the SPR spectroscopy there exist three techniques which can be used to determine both the thickness and refractive index of a thin film, namely the two-thickness, two-media and two-color methods [16–18]. The first method is not applicable in the present case, since SAMs of AuNPs with different thicknesses $< 2r >$ could be realized only by the deposition of nanoparticles with different diameter. The second method consists in the measurement of the SPR reflectivity spectra of the sample after the deposition of the AuNPs using two different external media. This technique is not the most appropriate for our application, since the change of the external liquid medium after the deposition of the metal nanoparticles might influence the strength of electrostatic interaction between the amino group of APTMS and the negative charges of the AuNPs, with possible leaching of the metal particles from the SiO_2 surface to the new liquid environment. The third technique is effective when the ratio of the refractive indices of the thin film at two different wavelengths is known. Looking at Eq. (1), it would appear that in our case the application of the third method is not possible because the parameter f is not known. Anyway, when considering the condition of very low the surface density ($f << \varepsilon_m', \sigma << \varepsilon_m'/< r >^2$), Eq. (1) can be simplified as

$$\varepsilon_{eff}' - \varepsilon_m' = f\left[\frac{(\varepsilon' - \varepsilon_m')C + \varepsilon'' D}{C^2 + D^2}\right], \varepsilon_{eff}'' \approx 0, \tag{5}$$

where the parameters A and B maintain their original expression as described by Eq. (2), while $C = \{\varepsilon_m' + (\varepsilon' - \varepsilon_m')/3\}$ and $D = \varepsilon''/3$. Hence, in the low surface density regime, when $\varepsilon_{eff}'' \approx 0$, it is possible to find an analytical relation for the ratio between the real part of ε_{eff} at two different wavelengths, which is now independent from metal filling factor f. In these conditions, two-color spectroscopy may be applied for the characterization of the AuNPs/water composite layer using the following dispersion relation:

$$Q_{\lambda_1,\lambda_2} = \frac{(\varepsilon_{eff}' - \varepsilon_m')_{\lambda_1}}{(\varepsilon_{eff}' - \varepsilon_m')_{\lambda_2}} = \frac{(\varepsilon' - \varepsilon_m')_{\lambda_1} \times C_{\lambda_1} + (\varepsilon'' \times D)_{\lambda_1}}{(\varepsilon' - \varepsilon_m')_{\lambda_2} \times C_{\lambda_2} + (\varepsilon'' \times D)_{\lambda_2}} \times \frac{C_{\lambda_2}^2 + D_{\lambda_2}^2}{C_{\lambda_1}^2 + D_{\lambda_1}^2} \tag{6}$$

where λ_1 and λ_2 represent the experimental excitation laser wavelengths.

The electron mean free path limitation has to be taken in account for the correct determination of the dielectric constant of the AuNPs when the dimension of the nanoparticles under analysis is of the order or less than about 15 nm, but has no influence on the dielectric constant for nanoparticles of higher dimensions, as explained in [12]. We point out that the theoretical model described above and the final Eq. (6), which represent the base

Optics EXPRESS

of the presented optical method, are completely independent from the electron mean free path assumption, and their validity is not restricted to a particular dimension of the AuNPs.

4. Results and discussion

4.1 Comparative measurements

Typical TEM and AFM images used for the comparative analysis of the dimension of the AuNPs are shown in Figs. 2(a) and 2(b), respectively. In the latter case, data analysis was carried out considering only the height of the nanomaterial, using Nanoscope Analysis software, version 1.4, by Bruker. The corresponding experimental statistical size distributions are represented in the inset of the figures. In all the cases, the size distribution is modelled using a normalized log-normal function [19]

$$n(r) = \frac{1}{\sqrt{2\pi} w r} e^{\frac{-[\ln(r) - \ln(r_c)]^2}{2w^2}} \tag{7}$$

where the function parameters w and r_c are linked to the values of $< r >$ and of the statistical standard deviation δ by the relations $< r >= e^{M + \frac{w^2}{2}}$ and $\delta = (e^{w^2 + 2M}(e^{w^2} - 1))^{\frac{1}{2}}$, where $M = \ln(r_c)$.

The same approach has been applied for the determination of $< r >$ and δ using the statistical size distribution obtained by DLS. In Table 1, the values of the statistical mean radius $< r >$ and standard deviation δ of the size distribution of the AuNPs are listed, as determined by the use of the different characterization techniques. The $< 2r >_{DLS}$, as usually overestimates the real average diameter of the AuNPs, which is more conveniently determined using the statistical distribution of sizes obtained from TEM or AFM analysis.

Before applying the two-color method on our colloidal dispersion of AuNPs, we verified experimentally the qualitative overlap between the resonances in the extinction cross-section of the nanomaterial and the spectral position of the exciting wavelengths used experimentally, λ_1 = 633 nm and λ_2 = 783 nm. Figure 2(c) represents the experimental extinction spectra of the colloidal dispersion of AuNPs, together with the theoretical fit of Mie with both dipolar and quadrupolar orders [19], obtained using the TEM statistical distribution shown in Fig. 2(a). In the figure are also represented two vertical lines, corresponding to the excitation wavelengths used in our experimental configuration. The overlap between the experimental and theoretical extinction spectra is excellent, confirming that the TEM size distribution and the value of $< r >_{TEM}$ of Table 1 are reliable, so that will be considered as our reference data in further discussion. Moreover, the lines corresponding to λ_1 and λ_2 are considerably far from the LSPR band of the gold colloids, so that the single isolated AuNP can be reasonably considered as transparent, as demonstrated in details in Section 4.4.

Table 1. Mean value $< r >$ and standard deviation δ of the statistical distribution of radius of the citrate stabilized AuNPs measured using different experimental techniques.

Techniques	DLS	TEM	AFM
Radius ($< r >$)	8.8 nm	7.4 nm	7.3 nm
Standard deviation (δ)	2.7 nm	1.5 nm	1.2 nm

Optics EXPRESS

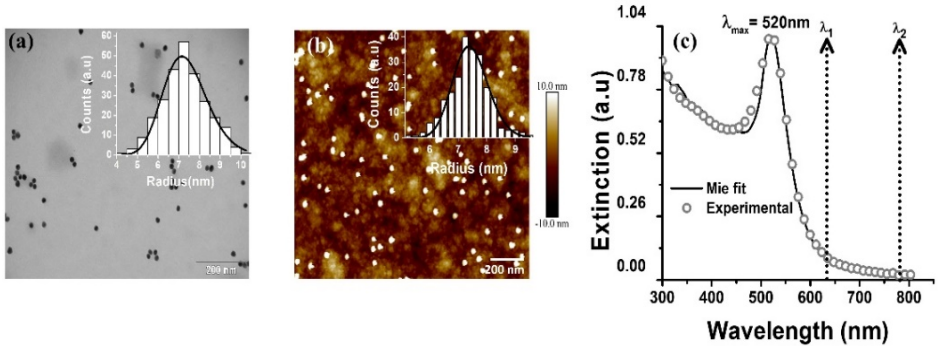

Fig. 2. (a) TEM image of the AuNPs and (b) AFM image on 1 μm x 1 μm region of APTMS functionalized SiO_2 thin film surface after interaction with the AuNPs. The inset of the images show the statistical AuNPs size distribution obtained using (a) TEM and (b) AFM microscopy over a set of 400 data points. Log normal distribution is used to obtain the best fit on the experimental statistical distribution, represented as continuous line. (c) Comparison between the experimental (open grey circles) and theoretical (continuous black line) extinction spectra of the colloidal dispersion of AuNPs in water. The fit on the experimental data and the theoretical curves were obtained applying the Mie theory with both dipolar and quadrupolar orders [19]. The vertical dashed lines represent the experimental excitation wavelengths used for the demonstration of the two-color SPR nanosizer.

4.2 Two-color SPR spectroscopy

The sensing of the AuNPs in the low density regime was performed over a 30 nm thick SiO_2 thin film, to optimize the sensitivity enhancing the spatial overlap between the SPR evanescent wave and the nanomaterial [6]. Before the deposition of the SAM of AuNPs, the Au/SiO_2 bilayer constituting the optical sensing platform is characterized by two-color SPR spectroscopy using the experimental procedure described in [11], in order to retrieve the values of both the refractive index and the thickness of gold and SiO_2 thin film at both laser radiation wavelengths. In Table 2 we summarize the results obtained at the excitation wavelengths of λ_1 = 633 nm and λ_2 = 783 nm. The refractive index of the liquid environment in contact with the AuNPs deposited over the SiO_2 surface can be considered as the one of pure water, since the excess of citrate in the colloidal suspension of nanomaterial was previously eliminated by centrifugation process, and the final reflectivity measurements is performed after rinsing the sample with ultrapure water.

Table 2. Experimental values of the optical parameters of the SPR sensing platform obtained using the experimental procedure described in [11]. The refractive index of water and SF4 were taken from [20].

λ (nm)	SF4	Gold		SiO_2		water
	ϵ_r	t(nm)	$\epsilon = \epsilon_r + i\,\epsilon_i$	t(nm)	ϵ_r	ϵ_r
633	3.06 [20]	49.8	−11.91 + i1.51	29.12	2.15	1.77 [20]
783	3.02 [20]	49.8	−23.48 + i1.79	29.12	2.13	1.76 [20]

Figure 3(a) represents the experimental SPR reflectivity curves of the Au/SiO_2 sensing platforms in water at the excitation wavelengths λ_1 and λ_2, before and after the deposition of the SAM of AuNPs. Therein, for each wavelength λ we indicate the shift in the angle of resonance $\Delta\theta_\lambda^{SPR}$ in the SPR curves upon the deposition of the Au/water composite thin film. As explained in [16,17,18], to each $\Delta\theta_\lambda^{SPR}$ it is associated a continuous line in the plane ε_{eff} Vs $< r >= t_{eff}/2$, composed by the couples of values of the dielectric constant

Optics EXPRESS

and thickness of the thin film under investigation which induce the angle shift observed experimentally.

For calculation of the lines in the plane ε_{eff} Vs $< r >= t_{eff}/2$ associated to the experimental SPR spectra, we developed a code using the software MatLab 9.0 based on the classical transfer matrix method [21], which calculates the reflectivity curves of planar multi-layer systems. In the code we fix the values of the parameters of the Au/SiO_2 bilayer as listed in Table 2, and vary the values of ε_{eff} and t_{eff} of the Au/water composite thin film to match the experimental angle of resonance shift $\Delta\theta_{\lambda}^{SPR}$. The results are shown in Fig. 3(b), where the filled black and grey points represent the solutions relative to the wavelengths λ_1 and λ_2, respectively. The intersection point of the curves highlighted in the figure represents the final measured value of both t_{eff} and ε_{eff}, obtained by shifting the curve associated to λ_2 using the parameter $Q_{\lambda_1,\lambda_2} = 1.266$ calculated from Eq. (5) The value of the mean radius of the AuNPs estimated by SPR spectroscopy is $< r >_{SPR} = 7.1nm$, which matches with an accuracy better than *0.5* nm with the results obtained by TEM and AFM analysis reported in Table 1, considered as reference results.

Once determined the average radius $< r >_{SPR}$, we combine Eqs. (1) to (4) together with the value of the effective dielectric constant $\varepsilon_{eff} - \varepsilon_m = 0.0152$ measured in Fig. 3(b), and calculate the value of *f* using the following relation:

$$f = \frac{(\varepsilon'_{\text{eff}} - \varepsilon'_m)\,(\varepsilon_i^2 + \varepsilon_r^2 + 4(\varepsilon_r + \varepsilon'_m))}{3(\varepsilon_i^2 - 2\varepsilon'^2_m + \varepsilon_r(\varepsilon_r + \varepsilon'_m))} \tag{8}$$

By Eq. (8) we obtain $f = 0.0031$ and $\sigma_{SPR} = 27NP/\mu m^2$, in good accordance with the average surface density of about $25NP/\mu m^2$ as determined afterwards by AFM control measurements executed over the same sample.

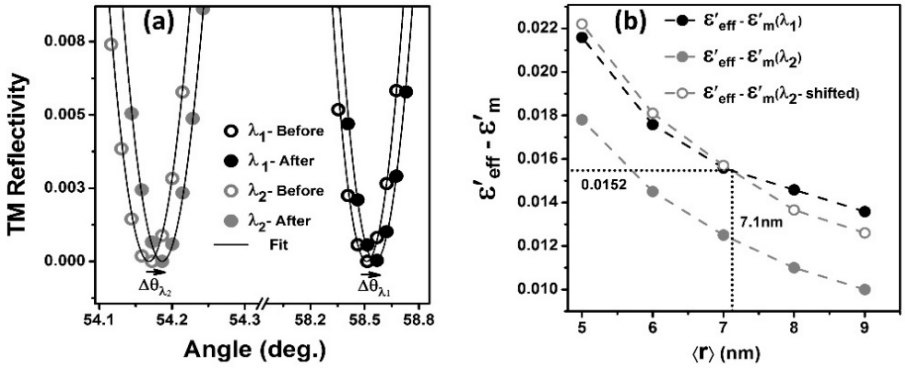

Fig. 3. (a) Experimental SPR minimum angle profiles at λ_1 (black) and λ_2 (grey) before (open circles) and after (fill circles) the deposition of the SAM of AuNPs. The observed SPR angle shift are $\Delta\theta_{\lambda 1} = 0.0471°$ and $\Delta\theta_{\lambda 2} = 0.0186°$. (b) Curves of the possible values in the plane ε_{eff} Vs $<r> = t_{eff}/2$ at the wavelengths λ_1 and λ_2. The intersection point of the curves represents the real value, obtained by shifting the curves using the parameter $Q_{\lambda_1,\lambda_2} = 1.266$ calculated from Eq. (5).

4.3 Accuracy evaluation

In a previous work [16] we evaluated that the accuracy $\delta\epsilon_r$ in the determination of the real part of the dielectric constant of the gold thin film supporting the plasma wave is about 0.5%, and

Optics EXPRESS

represents the main source of experimental error in the determination of the optical constants and thickness of the composite AuNP/water thin film. Indeed, the uncertainty $\delta\epsilon_r$ propagates, and influences the determination of the crossing point of the curves of the possible values in the plane ε_{eff} Vs <r> = $t_{eff}/2$ at the wavelengths λ_1 and λ_2 (Fig. 3(b)). To determine the value of $\Delta r_{experimental}$ we found the new intersection point in the plane ε_{eff} Vs $< r >= t_{eff}/2$ at the wavelengths λ_1 and λ_2 by changing the value of the dielectric constant of the gold thin film supporting the plasma wave by $\delta\epsilon_r = \pm 0.5\%$. The new curves in the ε_{eff} Vs $< r >= t_{eff}/2$ plane are represented in Fig. 4. From the results shown in the latter, we conclude that the experimental accuracy in the determination of the main radius by SPR spectroscopy is ± 0.5 nm, corresponding to $\Delta r_{experimental} \approx 7\%$.

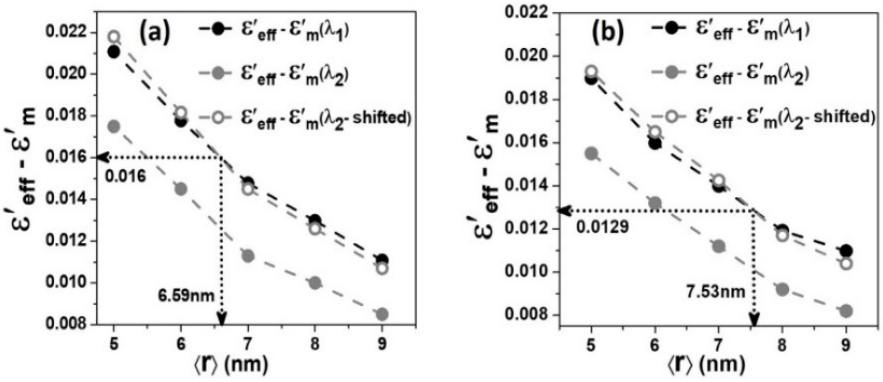

Fig. 4. Curves in the plane ε_{eff} Vs $< r >= t_{eff}/2$ corresponding to a variation $\delta\epsilon_r$ of the dielectric constant of the thin layer of gold supporting the plasma wave. (a) + 0.5%, (b) – 0.5%. The experimental accuracy in the determination of the main radius by SPR spectroscopy is ± 0.5 nm, corresponding to $\Delta r_{experimental} \approx 7\%$.

Anyway, other factors such as the polidispersitivity of the colloidal solution of AuNPs and nanoparticle surface density in the composite thin film, have further influence in the accuracy of the result. To determine the dependence of the accuracy of the measurement of the mean size of the AuNPs on the surface density σ, we first used our code to calculate the theoretical value of the shift in SPR angle $\Delta\theta_\lambda^{SPR}$ associated to the deposition of an array of spherical, identical and perfectly monodispersed AuNPs with the radius equal to $<r>_{TEM}$ = 7.4 nm. The calculus was repeated by fixing the values of the parameters of the Au/SiO_2 bilayer as listed in Table 2, and considering increasing values of σ up to about 150 NP/μm^2. For each value of surface density, we calculated the solution lines in the plane ε_{eff} Vs <r>, and found the final value $<r>_{SPR}$ by shifting the curve associated to λ_2, accordingly to Eq. (5). Figure 5(a) shows the theoretical percentage deviation $\Delta r_{density}$ between $< r >_{TEM}$, considered as the reference value, and $< r >_{SPR}$ obtained by the theoretical application of the two-color method in the low surface density approximation. The results demonstrate that the accuracy scales almost linearly with σ, rising up to 10% for densities higher than ~100 NP/μm^2, but being as small as 2% when working with NPs surface densities $\sigma \le 20\, NP/\mu m^2$ ($f \le 2.5\times10^{-3}$), a condition which we demonstrated experimentally.

The colloidal dispersion of AuNPs is not perfectly monodispersed, coherently with the results reported in Table 1. Independently from the actual surface density σ, the real metal volume factor of the AuNPs array is different from the one calculated using the approximate expression $f = 2\pi < r >^2 \sigma / 3$, and depends on the size distribution parameter δ. To understand the effect of the polidispersitivity on the SPR spectra, we define a relative radius

Optics EXPRESS

standard deviation $\delta_{rel} = \delta / < r >$, and consider trials colloidal dispersions of AuNPs characterized by a normalized log-normal statistical distributions $n(r)$ with increasing δ_{rel} ranging between 0% and 90%. Considering for example the distribution obtained by the TEM measurements, we have $< r >_{TEM} = 7.4nm$ and $\delta_{TEM} = 1.5nm$, corresponding to a relative standard deviation $\delta_{rel} = 20\%$.

We evaluate theoretically the effect that the statistical size dispersion of the AuNPs has on the SPR curves defining a statistical metal volume filling fraction as

$$f_{Stat} = \frac{\mathrm{N} < V_P >}{\mathrm{V_{CL}}} = \frac{\sigma < V_P >}{2h} = \frac{2\pi\sigma}{3h} \int_0^h r^3 \, n(r) \, dr \tag{9}$$

where *n(r)* is given by Eq. (7), V_{CL} is the volume of the thin composite layer of height *2h* over the SiO_2 thin film, $<V_P>$ is the statistical mean volume of a single nanoparticle, and N is the total number of AuNPs interacting with the SiO_2 surface (σ = N/A). The value of σ is maintained constant to 10 NP/μm^2, in order to fulfil the low surface density condition. After putting Eq. (7) in Eq. (9), we get

$$f_{Stat} = \frac{\sqrt{2\pi}\sigma}{3wh} \int_0^h r^2 \, e^{\frac{-[\ln(r) - \ln(r_c)]^2}{2w^2}} \, dr \tag{10}$$

From Eq. (7), the ratio of the population of AuNPs with radius r_c and radius equal to *h* is given by

$$\frac{n(h)}{n(r_c)} = e^{-[\ln(\frac{h}{r_c})]^2} = e^{-n} \tag{11}$$

Defining $y = \ln(h/r_c)$, Eq. (11) reduces to the equation of second order $y^2 + 2w^2 y - 2w^2 n = 0$, which leads to the solution

$$h = r_c \, e^{-w^2 + \sqrt{2nw^2 + w^4}} \tag{12}$$

The choice of the thickness *2h* of the composite layer, defines the maximum dimension of the nanoparticle that we are taking in account to calculate the statistical filling factor. For the present case, we defined *h* considering n = 2, so that *h* corresponds to the radius of AuNPs with a population e^{-2} smaller than the population of nanoparticles with radius r_c.

When considering f_{stat} instead of *f*, the theoretical angle shift $\Delta\theta_{\lambda}^{SPR}$ upon interaction between the SiO_2 surface and the AuNPs is different from the angle shift obtained considering the array distribution of nanoparticles with the same surface density σ but constituted by identical AuNPs with radius equal to $<r>_{log\text{-}normal}$, which is the statistical main radius calculated from the trial log-normal distribution $n(r)$. For each value of δ_{rel}, we used our code to calculate $\Delta\theta_{stat}^{SPR}$ and the corresponding solution lines in the plane ϵ_{eff} Vs <r>, and found the final value $<r>_{SPR}$ by shifting the curve associated to λ_2 accordingly to Eq. (5). The results are summarized in Fig. 5(b), where we represent the theoretical percentage deviation $\Delta r_{dispersion} = 100(<r>_{SPR} - <r>_{log\text{-}normal})/(<r>_{log\text{-}normal})$ depending on the parameter δ_{rel}. In the latter expression, $<r>_{log\text{-}normal}$ is the reference value of the main radius, and $<r>_{SPR}$ is the value of the main radius obtained by the application of the two-color method in the approximation of monodispersed colloidal solutions.

Optics EXPRESS

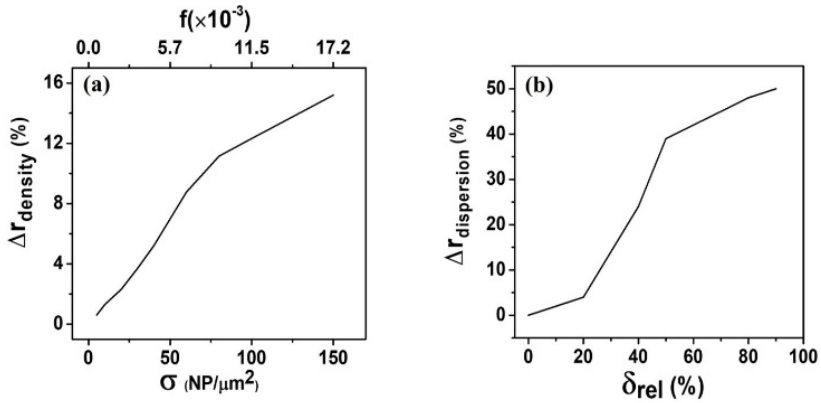

Fig. 5. (a) Percentage deviation $\Delta r_{density}$ between the value $\langle r \rangle_{TEM}$ and the value of the average radius $\langle r \rangle_{SPR}$ obtained by the application of the two-color method depending on σ. (b) Percentage deviation $\Delta r_{dispersion}$ between $\langle r \rangle_{log\text{-}normal}$ and $\langle r \rangle_{SPR}$ obtained by the application of the two-color method depending on the relative radius standard deviation $\delta_{rel} = (\delta_{log\text{-}normal}/\langle r \rangle_{log\text{-}normal})$.

One can see that when the value of δ_{rel} is between 0% and 20%, which is the typical range of colloidal dispersions of AuNPs synthesized by wet chemical methods or pulsed laser ablation in liquids (PLA) [22,23], $\Delta r_{dispersion}$ is lower than 4%. We conclude that two-color SPR spectroscopy can be used in a very low surface density regime ($f \leq 4 \cdot 10^{-3}$, $\sigma \leq 20$ NPs/μm^2) for the determination of the average dimension of spherical AuNPs with a mean diameter of the order of 15 nm with an accuracy $\Delta r = (\Delta r_{dispersion} + \Delta r_{density} + \Delta r_{experimental})$ better than ~10%, when considering monodispersed nanoparticles (i.e $\delta_{rel} = 0$). In the same surface density conditions, when δ_{rel} of the size distribution of the colloidal AuNPs is lower than 20%, the average radius of the NPs can be measured with a relative accuracy Δr better than ~15%. The presented theoretical calculations, show that the influence of the experimental parameters (surface density, polidispersitivity, $\delta\epsilon_r$) on the accuracy of the method cannot be ruled out, and validate the optical method when the effective accuracy in the discrimination of AuNPs of different sizes can be maintained in the order of ~10 to 15%.

4.4 Limits of applicability of two-color SPR nanosizer

At the base of the reliability of the presented optical method is the validity of the Maxwell-Garnett (MG) theory. The hardest restriction in the use of the effective medium theories is related to the dimension of the nanoparticles included in the transparent dielectric matrix, since the scattering cross-section of the nanoparticles is neglected in the formulation of the effective dielectric constant ε_{eff} of the composite thin film [15,19]. When the exact shape and spectral position of the maximum of the absorption cross-section of the composite thin film is desired, MG theory can be used for AuNPs with a mean diameter up to ~10 nm, while modified generalized Maxwell-Garnett Mie (MGM) theory can be used with reliable predictions up to nanoparticles diameters of ~40 nm [24]. In any case, when the scattering process of the isolated single AuNP is not negligible in the expression of the extinction cross-section σ_{ext}, all the effective medium theories lose their physical meaning, as pointed out in [25]. As reported in [15], the formulation of the MG theory used in the present research makes use of the quasi static approximation with dipolar fields, and includes in the expression of ε_{eff} additional parameters taking in account the effects that the geometry and the dimension (up to ~50 nm) of AuNPs have on the spectral position and the intensity of the absorption cross-section, respectively. This linear dimension upper limit of about 50 nm, includes the range of dimension commonly used in both PA-SPR spectroscopy [3] and bio-related applications [1].

Optics EXPRESS

The solution that we propose in the present research to overcome the limits of effective medium theory in the prediction of the extinction properties of composite thin films, is to consider samples with negligible optical density, so that $\varepsilon''_{eff} \approx f \approx 0$. The latter condition can be reached by probing the composite thin film with an excitation wavelength as far as possible from the LSPR resonances of the arrays of nanoparticles, and by the deposition of SAM of AuNPs with low surface density σ.

In fact, the optical density $\tau(\lambda, \sigma)_{SAM}$ for a SAM of monodispersed AuNPs with surface density σ and thickness (i.e diameter) *2r* can be simply written as

$$\tau(\lambda,\sigma,r)_{SAM} = (\log e)\frac{N}{V}\sigma_{ext}(\lambda,r)\cdot 2r = (\log e)\sigma\cdot\sigma_{ext}(\lambda,r) \qquad (13)$$

where λ is the excitation wavelength, σ_{ext} is the extinction cross-section of the isolated AuNP, and *N* is the total number of nanoparticles contained in the volume *V = 2rA*.

As shown in Fig. 2(c), the wavelengths λ_1 and λ_2 used experimentally in the present research are reasonably far from the LSPR resonance of the colloidal solution of AuNPs. The optical densities of the composite monolayer calculated by Eq. (13) at the experimental surface density of 27 NP/μm^2 are $\tau_{\lambda 1} \approx 2.0 \times 10^{-4}$ and $\tau_{\lambda 2} \approx 3.5 \times 10^{-5}$. In these conditions, both the absorption and the scattering by the composite thin film are negligible (i.e $\varepsilon''_{eff} \approx 0$). Hence, the MG theory is used only to predict the effect that nanosized inclusions have on dispersion properties of the real part of effective dielectric constant of the thin film, using the expression of ε'_{eff} at the first order in *f* like in Eq. (5).

When negligible extinction of the SAM of AuNPs can be considered, the real part of the effective refractive can be written as $n_{eff} = (n_{water} + \Delta n)$, where $\Delta n << 1$, and it holds the following relation for the real part of the effective dielectric function:

$$\varepsilon_{eff} = n_{eff}^2 - \kappa_{eff}^2 \approx n_{water}^2\left(1+\frac{2\Delta n}{n_{water}}\right) - \kappa_{eff}^2 = n_{water}^2 + (2n_{water}\Delta n - \kappa_{eff}^2) \qquad (14)$$
$$\varepsilon_{eff} \approx n_{water}^2 + 2n_{water}\Delta n$$

where in the last passage it was considered that $\kappa_{eff}^2 << 2n_{water}\Delta n$.

Using Eqs. (5) and (14) it is straight to calculate that in the experimental condition used during our measurement (<2r> ~15 nm, σ = 27 NP/μm^2) we have $2n_{water}\,\Delta n_{633nm} \approx 1.7\,x\,10^{-2}$, corresponding to $\Delta n_{633nm} \approx 6.2\,x\,10^{-3}$. It appears now clear that in the conditions of very low τ, SPR spectroscopy in the Kreschtmann configuration is particularly suited for the present optical investigation, due to its recognized high sensitivity in the detection of surface analyte interactions and small refractive index changes at the metal-dielectric interface [26].

Here we point out that when considering a SAM of AuNPs of radius *r* Eq. (13) can be manipulated to obtain the relation

$$2\frac{\omega}{c}\kappa_{eff} = e(\lambda) = \frac{\sigma\,\sigma_{abs}}{<2r>} < \frac{\sigma\,\sigma_{ext}}{<2r>} \qquad (15)$$

where e(λ) is the extinction coefficient of the thin film. Strictly, the connection between κ_{eff} and e(λ) expressed by Eq. (15) is valid only for homogeneous materials with negligible scattering effects, since κ_{eff} only takes in account for the absorption of the material. Since the scattering of the electromagnetic wave by the nanoparticles represents a loss channel not considered mathematically in the formulation of the MG theory, it holds the in Eq. (15). Using the Mie theory to calculate σ_{ext} in the latter inequation, it is straightforward to

Optics EXPRESS

demonstrate that in our experimental conditions we have $\kappa_{eff}^2(633\,nm) < 5\,x\,10^{-7}$, so that the approximation $\kappa_{eff}^2 << 2n_{water}\Delta n$ expressed by Eq. (14) is largely satisfied.

Equation (13) gives important information about the procedure to be followed to deposit SAM of AuNPs with the same optical density using nanoparticles of different radius *r*. Considering the scaling relation between σ and σ_{ext}, when the dimension of the AuNPs increases we can maintain a low value of τ by decreasing the surface density σ. The scaling between $\sigma(r)$ and the dimension of the monodispersed AuNPs is shown in Fig. 6(a), where the reference experimental value $\tau_{\lambda 1}$ was considered. The scaling is shown for mean radius ranging from 7 to 30 nm, and the extinction cross-section σ_{ext} (633 nm, *r*) of the single nanoparticle was calculated applying the Mie theory with both dipole and quadrupole oscillations [19]. In the same graph, for each value of nanoparticle surface density and radius, is represented the corresponding mass surface density of gold, calculated as $\sigma_{mass}(r) = \sigma(r)\,\rho_{Au}\,r^3$, where ρ_{Au} = 19.32 g/cm^3 is the bulk density of gold. In Fig. 6(b) are represented, for both wavelength λ_1 and λ_2, the theoretical shift of the SPR angle $\Delta\theta\,(r, \sigma(r))$ associated to the deposition of a SAM of AuNPs with the calculated mass surface density $\sigma_{mass}(r)$, where the effective dielectric constant of the composite layer has been calculated by the use of Eq. (5). In Fig. 6(b) the horizontal dashed red-line, line is set in correspondence of $\Delta\theta_{SPR}$ = 0.01°, corresponding to a conservative value of the angular resolution of traditional or commercial SPR spectrometer, in terms of minimal observable angular shift [26].

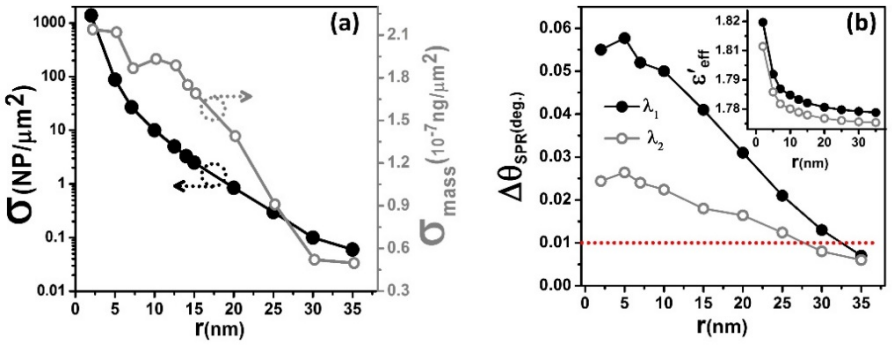

Fig. 6. Theoretical behaviour of SAM of monodisperse AuNPs with same optical density $\tau \approx \tau_{\lambda 1}$. (a) Surface density $\sigma(r)$ (black points, left Y-axes) and mass surface density of gold $\sigma_{mass}(r)$ expressed in ng/μm^2 (grey circles, right Y-axes) in function of the radius *r* of the AuNPs. (b) Shift of the angle of resonance $\Delta\theta\,(r)$ at both the excitation wavelengths λ_1 (black points) and λ_2 (grey circles) after the deposition of the associated mass surface density of gold $\sigma_{mass}(r)$. The dashed horizontal red-line is set in correspondence of $\Delta\theta_{SPR}$ = 0.01°.

As evident in Fig. 6(a), to maintain a reference value of optical density of the SAM of $\tau_{\lambda 1} \approx 2.0 \times 10^{-4}$ for AuNPs up to diameters of the order of 60 nm, it is necessary to deposit SAM with a surface density of the order of 0.1 NP/μm^2. In this way, with the increasing of the linear dimension, the mass of gold deposited in form of nanoparticles on the SiO_2 surface decreases, ultimately approaching the range of 10^{-18} ng/μm^2. A similar trend is observed in the theoretical angle shift $\Delta\theta_{SPR}$ after the deposition of the SAMs of AuNPs, reported in Fig. 6(b). In the low surface density approximation, when the refractive index of the composite layer can be approximated as purely real, the surface mass density and the SPR angular shift are linearly proportional one with each other, and the two-color nanosizer can be considered as an accurate nanobalance, with a maximum response for SAM of AuNPs with a mean radius of the order of 15 nm, corresponding to a maximum mass surface density of gold of about 2 x10 $^{-17}$ ng/μm^2. The smallest angle shifts $\Delta\theta_{SPR}$, observed at the wavelength of 783 nm for nanoparticles with a radius of 30 nm, is of the order of 0.005° degrees, corresponding to the double of the angular resolution of our experimental set-up, in terms of minimal

Optics EXPRESS

observable angular shift. Increasing the dimension of the nanoparticles, Eqs. (5) and (15) evidence that both κ_{eff} and Δn tends to 0, as shown from the behaviour of the effective dielectric constant represented in the inset of Fig. 6(b). Nevertheless, it is straightforward to verify that the condition $\kappa_{eff}^2 << 2n_{water}\Delta n$ it is largely satisfied also for the largest nanoparticles (r = 30 nm), since $2n_{water}\,\Delta n_{633nm} \approx 7.0x10^{-3}$ and $\kappa_{eff}^2(633nm) < 1.4x10^{-6}$. Hence, under the proper experimental restrictions on the optical characteristics of the deposited SAM of AuNPs, the condition of transparency expressed by Eq. (14) may be correctly satisfied independently from the mean radius of the AuNPs to be analysed, and the refractive index of the effective composite layer can be reliably approximated as purely real.

It should be mentioned that when considering AuNPs with increasing dimension, dipole-dipole interparticle resonances might be taken in account for the accurate determination of $\Delta r_{density}$ Vs σ (Fig. 5(a)). For example, near-field dipole-dipole interaction between adjacent gold nanoparticles with a diameter of 50 nm, set-on at interparticle average distance <*d*> of about 100 nm. Anyway, due to the $<d>^{-3}$ dependence of the near-field interaction, its effect is negligible for <*d*> bigger than ~130 nm, corresponding to σ ≤ 60 NP/μm^2 [27], which is a huge surface density in comparison with the reference value reported in Fig. 6a for AuNPs of the same dimensions.

Concerning the possible contact and charge transfer between the AuNPs deposited over the SiO_2 surface of the SPR sensing platform, with formation of agglomerated clusters or even fractals, we underline that this phenomenon may be observable experimentally mainly when the SiO_2 surface is not functionalized by APTS or other molecular ligands for AuNPs [28]. In case of correct chemical functionalization of the SiO_2 surface, agglomeration of the AuNPs can be observable only at very high values of surface densities, which is the opposite case to the one considered in the present research, based on the assumption of low values of σ. For example, in a recent work multimodal dielectric-loaded waveguides (DLWGs) with SiO_2 external surface have been successfully used for the correct counting of AuNPs with characteristics similar to the ones used in the present research, without any sign of agglomeration up to surface densities of about 200 NP/μm^2 [29].

On the basis of our theoretical calculations, we conclude that the experimental configuration of the two-color SPR nanosizer proposed in the present research, is suitable for the measurement of the mean radius of AuNPs in the approximate range between ~2 and ~30 nm. The first limit is dictated by the setup of the electron quantum confinement [14], while the latter depends on the angular resolution of the two-color SPR nanosizer, since SAM of AuNPs with a low value of optical density and increasing linear dimension may be obtained only by a progressive decrease on the corresponding mass surface density of gold, with a decrease in the corresponding angle shift Δθ, as pointed out in Fig. 6(b). Since commercial or traditional SPR spectrometers based on angular interrogation in the Kreschtmann configuration are generally characterized by an angular resolution better than 0.01° [26], the results of Fig. 6(b) suggest that a conservative value of about 25 nm might be preferentially assumed as a realistic upper limit for a standard two-color SPR nanosizer.

4.5 Application of two-color SPR nanosizer to AuNPs of unknown dimensions

It is now possible to draw an out-line about the experimental procedure to follow for the correct application the two-color SPR nanosizer to citrate stabilized AuNPs of different dimensions. As briefly introduced at the end of Section 2, the principal experimental steps can be summarized as:

a) evaluation of the spectral overlap between the extinction cross-section of the AuNPs and the wavelength λ_1 and λ_2 of the excitation laser sources.

Depending on the experimental availability, λ_1 and λ_2 should be chosen as far as possible from the LSPR band of the single isolated spherical AuNP. From a

Optics EXPRESS

theoretical point of view, the excitation wavelengths of 633 and 783 nm used in the present work are suitable for the measurement of mean radius of AuNPs in the approximated range between ~2 and ~25 nm.

b) Accurate measurement of the dielectric constant and thickness of the gold and SiO_2 thin films constituting the SPR sensing platform, at both wavelengths λ_1 and λ_2.

The uncertainty of the values of the optical constants of the Au/SiO_2 bilayer is the major systematic error that influences the final accuracy in the performances of the SPR nanosizer, so that particular attention is suggested during the optical fabrication and SPR characterization of the sensing platforms [11,16].

c) Deposition of SAM of AuNPs with sufficiently low optical density τ.

As rule of thumb, considering the results represented in Fig. 6(b), using SPR Au/SiO_2 bilayers with the characteristics reported in the present research, the deposition of the AuNPs should be controlled in order to have a maximum SPR angle shift of the order of a few units of cents of degrees, in order to work in the conditions of transparency of the composite thin film, independently from the mean dimension of the AuNPs.

d) Analysis of the experimental data applying the two-color SPR method supported by MG theory in the low surface density approximation.

Interestingly, in the theoretical model exposed in Section 3 we didn't put any restriction to the chemical nature of the nanoparticle, but only the shape, supposed to be spherical. For material like metallic Cu, which present an LSPR band in the visible red region [19], other experimental configuration might be more suitable than the presented one. In this case, excitation laser sources in the near IR or IR region (i.e λ_1 = 783 nm, λ_2 = 1064 nm) might be preferred to minimize the overlap with the LSPR band of the isolated nanoparticle, although accurate calculation should be done in order to evaluate the sensitivity of the SPR sensors, which decreases with increasing wavelength [30]. The most serious restriction to the application of the two-color SPR nanosizer to nanomaterials of noble metals different from gold (i.e Ag,Cu) is the chemical activity of these species. In fact, the lack of control on their oxidation processes might infer to the nanomaterials optical properties that are not predictable by the use of the traditional Johnson and Christy datasheet [13], largely used from the scientific community for the modelling of the complex dielectric constant of the metals.

It is worth noting that the experimental step c) of the previous list is not trivial. The scaling represented in Fig. 6(b) between the surface density and the radius of the nanoparticle normally happens phenomenologically in experiments of PA-SPR spectroscopy [3]. In this case, the phenomenological scaling is due to the increase of the steric effects with the diameter of the nanoparticles, as reported in [3]. Unfortunately, there are not experimental reports that describe the same behaviour when the interaction between the external surface of the sensor and the AuNPs is not mediated by a bio-molecule, but using classical molecular ligands between gold and SiO_2, such as APTMS or MPTS. Vice versa, experimental studies about the interaction of citrate stabilized AuNPs of different dimensions with gold surfaces functionalized with 3-mercaptopropionic acid (MPA) or 2-mercaptoethylamine (MEA), reveal a progressive and faster broadening and shift of the SPR reflectivity spectra with increasing diameters [31,32], demonstrating that particular attention has to be taken for the control of the deposition of SAM of AuNPs with large dimension. The lack of information about the effect that the size of citrate stabilized AuNPs has on their association constant [33] with APTMS or MPTS, creates a reasonable doubt about the possibility to control easily the

Optics EXPRESS

deposition of SAM of AuNPs with progressively lower surface densities, as represented in Fig. 6(a).

Hence, after this fundamental optical study, our immediate goal is to investigate the extent at which the interaction between the molecular ligand deposited on the glass surface and the AuNPs is size dependent, in order to optimize the control on the optical density of the composite films. Multiple parameters may affect the interaction, such as the kind of molecular ligand between gold and SiO_2, its surface density on the SiO_2 thin film, the concentration of the colloidal solution of AuNPs, the pH of the water environment or the flux velocity of the AuNPs during the deposition over the functionalized glass surface. The control of the surface density should be obtained using a unique and well defined protocol for the chemical functionalization of the Au/SiO_2 bilayer, independent on the specific dimension of the AuNPs. This physico-chemical investigation goes beyond the scopes of the present research and represents the next step to be addressed for the practical application of the two-color nanosizer to gold nanostructures with dimension of several tens of nm.

5. Conclusions

We described both theoretically and experimentally the principle of work of a two-color SPR nanosizer applied to AuNPs. When the optical density of the Au/water composite film is negligible ($\sim 10^{-4}$ at 633 nm), the limitation of the MG theory in the prediction of the extinction properties of composite thin films is overcome, and the effective medium theory can be used reliably to predict the dispersion properties of the effective refractive index of the composite thin film, which can be approximated as purely real. This is demonstrated experimentally through the determination of the statistical mean size of a colloidal solution of polidispersed citrate stabilized AuNPs with a nominal diameter of ~15 nm. The experimental performances are comparable to expensive techniques such as AFM microscopy, DLS or TEM. When AuNPs of bigger dimension are considered, theoretical calculations show that the application of the two-color SPR nanosizer is only limited by the angular resolution of the SPR sensing platform, once the control of the optical density τ of the composite thin film is obtained by proper chose of the excitation laser wavelengths and the deposition of SAM of AuNPs with progressively lower mass surface density (i.e $\Delta\theta_{SPR}$). Since commercial or traditional SPR spectrometers with angular interrogation in the Kreschtmann configuration are characterized by a typical angular resolution better than ~0.01° [26], our theoretical results suggest that a standard configuration of a two-color SPR nanosizer in the visible range may be suited for characterization of AuNPs up to diameters of the order of ~50 nm. A dedicated physical-chemical investigation on the effect that the size of the gold nanoparticles has on the association constant with traditional $Au\text{-}SiO_2$ molecular ligands such as MPTS or APTMS is missing in literature, and will be addressed in the near future in order to verify the real extent at which the optical density of the SAM of AuNPs can be controlled to a low value when increasing the mean diameter of the nanoparticles. At the moment, this is the next step to be addressed for the application of the two-color nanosizer to nanoparticles with dimension of several tens on nm, which might be further extended to the characterization of gold nanoparticles with different shape, by proper modification of the theoretical polarizability, metal filling factor of the composite film, and the use of multimodal dielectric-loaded waveguides (DLWGs) to probe the anisotropy of the nanomaterial under study.

Funding

Instituto Nacional de Ciência e Tecnologia em Eletrônica Orgânica (INCT-INEO), Fundação Carlos Chagas Filho de Amparo à Pesquisa do Estado do Rio de Janeiro (FAPERJ), Fundação Amazônia Paraense de Amparo à Pesquisa (FAPESPA) and Conselho Nacional de Desenvolvimento Científico e Tecnológico (CNPq).

Optics EXPRESS

References

1. M. C. Daniel and D. Astruc, "Gold nanoparticles: assembly, supramolecular chemistry, quantum-size-related properties, and applications toward biology, catalysis, and nanotechnology," Chem. Rev. **104**(1), 293–346 (2004).
2. P. Eaton, P. Quaresma, C. Soares, C. Neves, M. P. de Almeida, E. Pereira, and P. West, "A direct comparison of experimental methods to measure dimensions of synthetic nanoparticles," Ultramicroscopy **182**, 179–190 (2017).
3. T. Špringer, M. L. Ermini, B. Špačková, J. Jabloňků, and J. Homola, "Enhancing sensitivity of surface plasmon resonance biosensors by functionalized gold nanoparticles: Size matters," Anal. Chem. **86**(20), 350–356 (2014).
4. Y. Uchiho, M. Shimojo, K. Furuya, and K. Kajikawa, "Optical response of gold-nanoparticle-amplified surface plasmon resonance spectroscopy," J. Phys. Chem. C **114**(11), 4816–4824 (2010).
5. A. Shiohara, Y. Wang, and L. M. Liz-Marzan, "Recent Approaches toward creation of hot spots for SERS detection," J. Photochem. Photobiol. Chem. **21**, 2–25 (2014).
6. M. S. Golden, A. C. Bjonnes, and R. M. Georgiadis, "Distance and wavelength dependent dielectric function of Au nanoparticles by angle-resolved surface plasmon resonance imaging," J. Phys. Chem. C **114**(19), 8837–8843 (2010).
7. N. Souza, J. Costa, R. Santos, A. Cruz, T. Del Rosso, and K. Costa, "Modal analysis of surface plasmon resonance sensor coupled to periodic array of core-shell metallic nanoparticles," *Resonance* (InTech, 2017).
8. J. Turkevich, P. C. Stevenson, and J. Hillier, "A study of the nucleation and growth processes in the synthesis of colloidal gold," J. Discuss. Faraday Soc. **11**, 55–75 (1951).
9. T. Del Rosso, Q. Zaman, M. Cremona, O. Pandoli, and A. R. J. Barreto, "SPR sensors for monitoring the degradation processes of Eu(dbm)3(phen) and Alq3 thin films under atmospheric and UVA exposure," Appl. Surf. Sci. **442**, 759–766 (2018).
10. I. Piwoński, J. Grobelny, M. Cichomski, G. Celichowski, and J. Rogowski, "Investigation of 3-mercaptopropyltrimethoxysilane self-assembled monolayers on Au(111) surface," Appl. Surf. Sci. **242**(1–2), 147–153 (2005).
11. T. Del Rosso, W. Margulis, G. Fontana, and I. C. S. Carvalho, *Metal Nanostructures for Photonics,* (Elsevier, 2018), Chap.10, pp. 223–259.
12. L. B. Scaffardi, N. Pellegri, O. Sanctis, and J. O. Tocho, "Sizing gold nanoparticles by optical extinction spectroscopy," Nanotechnology **16**(1), 158–163 (2005).
13. P. B. Johnson and R. W. Christy, ""Optical constants of the noble metals," Phys. Rev. B Condens," Matter Mater. **6**(12), 4370–4379 (1972).
14. U. Kreibig and C. V. Fragstein, "The limitation of electron mean free path in small silver particles," Z. Phys. **224**(4), 307–323 (1969).
15. M. A. García, J. Llopis, and S. E. Paje, "A simple model to evaluate the optical absorption spectrum for small Au-colloids in sol-gel films," Chem. Phys. Lett. **315**(5), 313–320 (1999).
16. T. Del Rosso, J. E. Sánchez, R. S. Carvalho, O. Pandoli, and M. Cremona, "Accurate and simultaneous measurement of thickness and refractive index of thermally evaporated thin organic films by surface plasmon resonance spectroscopy," Opt. Express **22**(16), 18914–18923 (2014).
17. H. E. de Bruijn, B. S. F. Altenburg, R. P. H. Kooyman, and J. Greve, "J. Greve, "Determination of thickness and dielectric constant of thin transparent dielectric layers using Surface Plasmon Resonance," Opt. Commun. **82**(5–6), 425–432 (1991).
18. K. A. Peterlinz and R. Georgiadis, "Two-color approach for determination of thickness and dielectric constant of thin films using surface plasmon resonance spectroscopy," Opt. Commun. **130**(4–6), 260–266 (1996).
19. M. Quinten, *Optical Properties of Nanoparticle Systems: Mie and Beyond* (Wiley, 2011).
20. M. N. Polyanskiy, "Refractive index database," https://refractiveindex.info.
21. L. M. Walpita, "Solutions for planar optical waveguide equations by selecting zero elements in a characteristic matrix," J. Opt. Soc. Am. A **2**(4), 595–602 (1985).
22. I. Capek, *Noble Metal Nanoparticles: Preparation, Composite Nanostructures, Biodecoration and Collective Properties* (Springer, 2017).
23. V. Amendola and M. Meneghetti, "Laser ablation synthesis in solution and size manipulation of noble metal nanoparticles," Phys. Chem. Chem. Phys. **11**(20), 3805–3821 (2009).
24. Y. Battie, A. Resano-Garcia, N. Chaoui, Y. Zhang, A. En Naciri, "Extended Maxwell-Garnett-Mie theory formulation applied to size dispersion of metallic nanoparticles embedded in host liquid matrix," J. Chem. Phys. **140**, 044705 (2014).
25. R. Ruppin, "Evaluation of extended Maxwell-Garnett theories," Opt. Commun. **182**(4–6), 273–279 (2000).
26. B. Liedberg, C. Nylander, and I. Lundström, "Biosensing with surface plasmon resonance--how it all started," Biosens. Bioelectron. **10**(8), i–ix (1995).
27. S. A. Maier, M. L. Brongersma, P. G. Kik, and H. A. Atwater, "Observation of near-field coupling in metal nanoparticle chains using far-field polarization spectroscopy," Phys. Rev. B Condens. Matter Mater. Phys. **65**(19), 193408 (2002).
28. M. Muniz-Miranda, T. Del Rosso T. Del Rosso, E. Giorgetti, G. Margheri, G. Ghini, and S. Cicchi, "Surface-enhanced fluorescence and surface-enhanced Raman scattering of push-pull molecules: sulfur-functionalized 4-

Optics EXPRESS

amino-7-nitrobenzofurazan adsorbed on Ag and Au nanostructured substrates," Anal. Bioanal. Chem. **400**(2), 361–367 (2011).
29. J. Souza, Q. Zaman, K.Q. Costa, V. Dmitriev, O. Pandoli, G. Fontes, and T. Del Rosso, "Limits of the Effective Medium Theory in Particle Amplified Surface Plasmon Resonance Spectroscopy Biosensors," to appear in Sensors (2019).
30. J. Homola, I. Koudela, and S. S. Yee, "Surface plasmon resonance sensors based on diffraction gratings and prism couplers: sensitivity comparison," Sens. Actuat. B. **54**(1-2), 16–24 (1999).
31. L. A. Lyon, M. D. Musick, P. C. Smith, B. D. Reiss, D. J. Pena, and M. J. Natan, "Surface plasmon resonance of colloidal Au-modified gold films," Sens. Actuat. B. **54**(1-2), 118–124 (1999).
32. L. A. Lyon, D. J. Pena, and M. J. Natan, "Surface plasmon resonance of Au colloid-modifiothered Au films: particle size dependence," J. Phys. Chem. B **103**(28), 5826–5831 (1999).
33. G. Margheri, S. Trigari, S. Sottini, R. D'Ágostino, T. D. Rosso, and M. D. Rosso, "The binding of EGFR to gm13 hosted in lipid raft-like biomembranes insighted by plasmonic resonance techniques," J. Sens. (2015), doi:10.1155/2015/282458.